Applied Mathematics and Computation 242 (2014) 528–540

Contents lists available at ScienceDirect

Applied Mathematics and Computation

journal homepage: www.elsevier.com/locate/amc

Heat and mass transfer of two-layer flows of third-grade nano-fluids in a vertical channel

U. Farooq [a], T. Hayat [c,d], A. Alsaedi [d], Shijun Liao [a,b,d,*]

[a] State Key Laboratory of Ocean Engineering, School of Naval Architecture, Ocean and Civil Engineering, Shanghai Jiao Tong University, Shanghai 200240, China
[b] MOE Key Lab in Scientific Computing, Shanghai Jiaotong University, Shanghai 200240, China
[c] Department of Mathematics, Quaid.i.Azam University, Islamabad 44000, Pakistan
[d] Nonlinear Analysis and Applied Mathematics (NAAM) Research Group, Faculty of Science, King Abdulaziz University, Jeddah 21589, Saudi Arabia

ARTICLE INFO

Keywords:
Two-layer flow
Third grade nano-fluid
Homotopy analysis method
BVPh 2.0

ABSTRACT

The heat and mass transfer of two-layer flows of non-Newtonian (third-grade) fluid in a vertical channel is investigated in details, when one layer of water is nano-fluid and the other is clear, with the viscous dissipation. In each layer, the boundary-layer flow is governed by coupled nonlinear ordinary differential equations (ODEs). The systems of coupled nonlinear ODEs are solved analytically by means of a Mathematica package BVPh 2.0 based on the homotopy analysis method (HAM), an analytic approximation method for highly nonlinear problems. The influence of the physical parameters is studied in detailed. It is found that the layer of nano-fluid has many different properties from that of clear fluid. This paper also illustrates the validity and power of the HAM-based Mathematica package BVPh 2.0 for some complicated boundary-layer flows.

1. Introduction

The mixed or combined convection arises in many situations such as, natural convection in the presence of ambient fluid circulations, the externally induced flow in heated channels, etc. The flow and heat transfer in mixed convection situations are topic of great interest due to its applications in chemical processing equipment, cooling of electronic circuitry by means of fan, solar technology, nuclear reactors cooled during emergency shut down, etc. Sparrow et al. [1] was the first to study the mixed convection flows, followed by Sparrow and Gregg [2], Tao [3], Szewczyk [4] and Merkin [5]. Due to its wide applications, a lots of investigations were made on fully developed mixed convection flows in a vertical channel. Rajagopal and Na [6] studied third-grade fluid between two infinite parallel vertical plates. Aung and Worku [7] investigated flows in a vertical channel with asymmetric wall temperature. Further, Aung and Worku [8] examined mixed convection flows in a vertical channel with different wall temperatures. They found that flow is reversed for large values of buoyancy parameter. Massoudi and Christie [9] studied the influences of the non-Newtonian nature of fluid on the skin friction and heat transfer. Barletta [10] investigated combined forced and free convection flows in a rectangular duct for laminar, fully developed regime. Boulama and Galanis [11] presented analytical solutions for fully developed mixed convection between parallel plates. Recently, Baoku and Olajuwon [12] investigated viscoelastic third-grade fluid past an infinite vertical insulated plate subject to suction across the boundary layer. Some more recent studies for flows of third-grade fluid can be consulted through the

* Corresponding author at: State Key Laboratory of Ocean Engineering, School of Naval Architecture, Ocean and Civil Engineering, Shanghai Jiao Tong University, Shanghai 200240, China.
E-mail address: sjliao@sjtu.edu.cn (S. Liao).

http://dx.doi.org/10.1016/j.amc.2014.05.126
0096-3003/

Refs. [13–18]. Note that the aforementioned studies investigate models with only a single-fluid. However, in practice, most of the problems relating to petroleum industry, geophysics, plasma physics, magneto-fluid dynamics, etc., involve multi-fluid flow situations. A number of complex interfacing transport phenomena may take place in non-isothermal multi-fluid systems. An important assumption usually met in these models is the interfacial thermal and chemical equilibrium between the fluids. Beckermann et al. [19] performed numerical investigation to analyze the flow and heat transfer between a fluid layer and a porous layer inside a rectangular enclosure. Kimura et al. [20] studied the influence of ratio of the depth of two-layers on the heat transfer. Malashetty et al. [21] presented analytical solutions for two region vertical enclosure with one region electrically conducting and the other electrically non-conducting. Kumar et al. [22] investigated the influences of the governing parameters on the flow and heat transfer for two-layer fluid with one region filled with micropolar fluid and the other with clear fluid. Umavathi et al. [23] examined three-layer flows with a porous media sandwiched between clear fluids. Nikodijevic et al. [24] obtained closed-form solutions for magnetohydrodynamic Couette flow of two immiscible fluids. Parthab et al. [25] studied two-layer mixed convective flow and heat transfer in a vertical channel with one region filled with conducting fluid and other with nonconducting ones.

Nanotechnology grows rapidly due to its immense applications in many electronic devices, vehicles, space craft, metrology, artificial organs and cooling applications of nano-fluids, and so on. Choi [26] is the first to use the term nano-fluid, who proposed that nanometer sized metallic particles can be suspended in industrial heat transfer fluids. Therefore, a nano-fluid is a suspension of nano-particles (metallic, non-metallic, or polymeric) in a conventional base fluid which enhances its heat transfer characteristics. Enhanced thermal properties of nano-fluids enable them to use in automotive industry, power plants, cooling systems, computers, etc. An in-depth review on nano-fluids can be found in the book by Das et al. [27] and in the review paper by Wang and Mujamdar [28]. Recently, the flows due to a mixed convection in a vertical channel in nano-fluids have drawn considerable attention. Kuznetsov and Nield [29] investigated natural convective boundary layer flows of a nano-fluid past a vertical plate. Xu and Pop [30] studied the influences of nano-particle volume fraction on the temperature and velocity distributions for fully-developed mixed convection flow in a vertical channel filled with nano-fluids. Gorsan and Pop [31] investigated mixed convection nano-fluid flow in a vertical channel for different physical parameters. Xu et al. [32] obtained series solutions for mixed convection flow of a nano-fluid in a vertical channel. Recently, Gorder et al. [33] investigated fully-developed two-layer fluid flows in a vertical channel with one region filled with nano-fluid and the other filled with clear fluid. In the same two-layer model by Gorder et al. [33], Farooq and Lin [34] proposed new non-dimensional quantities for physical parameters and exhibited the flow reversal phenomenon for sufficiently high buoyancy. Vajravelu et al. [35] investigated heat and mass transfer properties of three-layer fluid flow in which nano-fluid layer is squeezed between two clear viscous fluid.

To the best of our knowledge, the two-layer model with one region filled with non-Newtonian third-grade clear fluid and the other with non-Newtonian third-grade nano-fluid has never been investigated. Due to the non-Newtonian third-grade fluid, the flows are governed by more complicated, coupled ODEs in each layer. The systems of these coupled nonlinear ODEs are solved by means of the Mathematica package BVPh 2.0 [40], which is valid for nonlinear boundary-value or eigen-value problems with boundary conditions at multiple points, governed by coupled nonlinear ODEs. The BVPh 2.0 is free available online (http://numericaltank.sjtu.edu.cn/BVPh.htm). It is based on the homotopy analysis method (HAM) [36–39], an analytic approximation method for highly nonlinear problems. Unlike perturbation techniques, the HAM has nothing to do with small/large physical parameters, so that it is essentially a non-perturbation method. Besides, based on the homotopy in topology, the HAM provides us great freedom to choose the equation-type and base function of equations for high-order approximations. Especially, unlike all other analytic techniques, the HAM provides us a convenient way to control and adjust the convergence of solution series, so that the convergence of solution series can be guaranteed. Therefore, unlike other traditional analytic methods, the HAM is valid for highly nonlinear problems. The HAM has been widely applied to solve lots of nonlinear problems in science, engineering and finance. The BVPh 2.0 [40] is a HAM-based Mathematica package, which provides us an easy-to-use tool for nonlinear boundary-value or eigenvalue problems governed by coupled nonlinear ODEs.

In this paper, the complicated system of the coupled nonlinear ODEs in each layer of non-Newtonian fluid is solved conveniently by means of the BVPh 2.0. The influence of physical parameters on the flow, temperature, concentration, heat and mass transfer is investigated in detail. Reversed flow is observed for sufficiently large values of mixed convection parameter. These are helpful to deepen and enrich our understandings about the considered two-layer flows of third-grade fluid in a vertical channel.

2. Problem formulation

Consider steady-state, laminar, incompressible flow between two infinite vertical parallel plates extending in the x and z directions, with x-axis upwards and y-axis pointing to the right, as shown in Fig. 1. The region-I in the domain $0 \leqslant y \leqslant h$ is filled with a third-grade clear-fluid, and the region-II in the domain $-h \leqslant y \leqslant 0$ is occupied by a third-grade nano-fluid, respectively. In each layer, let ρ_i denote the density, μ_i the viscosity, α_i the thermal diffusivity and γ_i the non-Newtonian parameter, respectively, where $i = 1, 2$. The right and left walls have temperatures T_{w1} and T_{w2}, respectively. In the two regions, the fluid thermo-physical properties keep the same.

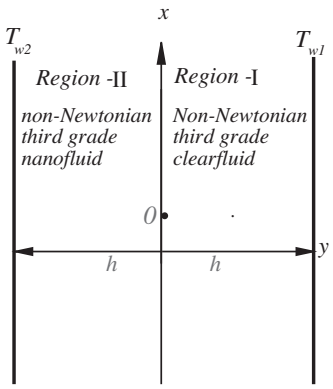

Fig. 1. Physical configuration.

Incompressibility condition is automatically satisfied and the governing equations of momentum, energy and nanoparticle volume fraction become:

(i) Region-I

$$\nu_1 \frac{d^2u_1}{dy^2} - \frac{1}{\rho_1}\frac{\partial p}{\partial x} + \frac{6\gamma_1}{\rho_1}\left(\frac{du_1}{dy}\right)^2 \frac{d^2u_1}{dy^2} + g\beta_1(T_1 - T_{w2}) = 0, \tag{1}$$

$$\alpha_1 \frac{d^2T_1}{dy^2} + \frac{\nu_1}{c_p}\left(\frac{du_1}{dy}\right)^2 + \frac{2\gamma_1}{\rho_1 c_p}\left(\frac{du_1}{dy}\right)^4 + \frac{Q_1}{\rho_1 C_p}(T_1 - T_{w2}) = 0. \tag{2}$$

(ii) Region-II

$$\nu_2 \frac{d^2u_2}{dy^2} - \frac{1}{\rho_2}\frac{\partial p}{\partial x} + \frac{6\gamma_2}{\rho_2}\left(\frac{du_2}{dy}\right)^2 \frac{d^2u_2}{dy^2} + g\beta_2(T_2 - T_{w2}) = 0, \tag{3}$$

$$\alpha_2 \frac{d^2T_2}{dy^2} + \frac{\nu_2}{c_p}\left(\frac{du_2}{dy}\right)^2 + \frac{2\gamma_2}{\rho_2 c_p}\left(\frac{du_2}{dy}\right)^4 + \tau\left[D_B\frac{dC}{dy}\frac{dT_2}{dy} + \frac{D_T}{T_{w2}}\left(\frac{dT_2}{dy}\right)^2\right] + \frac{Q_2}{\rho_2 C_p}(T_2 - T_{w2}) = 0, \tag{4}$$

$$D_B\frac{d^2C}{dy^2} + \frac{D_T}{T_{w2}}\frac{d^2T_2}{dy^2} = 0. \tag{5}$$

Here the subscripts $i = 1, 2$ denote the values for region-I and region-II, respectively. Moreover, u_i, v_i denote the x and y-component of fluid velocities, T_i the temperatures, Q_i the internal heat generation or absorption parameters, c_p the specific heat, ν_i the kinematic viscosities, β_i the coefficients of thermal expansion, g the gravitational acceleration, C the nano-particle volume fraction, D_B the Brownian diffusion coefficient, D_T the thermophoretic diffusion coefficient, and $\tau = (\rho C_p)_p/(\rho C_p)_f$ the heat capacity ratio, respectively. Here, the subscripts p and f respectively denote the nanoparticles and the base fluid.

Assume that the velocity, the shear stress, the temperature, and the heat flux at the interface are continuous. The no-slip boundary conditions require the x-component of the velocity to vanish at the wall. The boundary conditions on the temperature are isothermal. With these assumptions, the boundary and interface conditions for the problem are

$$\begin{cases} u_1(y) = 0, \quad T_1(y) = T_{w1}, & \text{at } y = h, \\ \left.\begin{array}{l} u_1(y) = u_2(y), \quad T_1(y) = T_2(y), \quad C(y) = 0 \\ \mu_1\frac{du_1}{dy} + 2\gamma_1\left(\frac{du_1}{dy}\right)^3 = \mu_2\frac{du_2}{dy} + 2\gamma_2\left(\frac{du_2}{dy}\right)^3, \quad k_1\frac{dT_1}{dy} = k_2\frac{dT_2}{dy}, \end{array}\right\} & \text{at } y = 0, \\ u_2(y) = 0, \quad T_2(y) = T_{w2}, \quad C(y) = C_w, & \text{at } y = -h, \end{cases} \tag{6}$$

where k_i $(i = 1, 2)$ are the thermal conductivities in the regions I and II. Following Buongiorno [41], we use the coupled Eqs. (1)–(5) for the nano-particle concentration. Define the following non-dimensional quantities

$$\begin{cases} y^* = \frac{y}{h}, \quad u_1^* = \frac{u_1}{\tilde{u}_1}, \quad u_2^* = \frac{u_2}{\tilde{u}_2}, \quad \theta_1 = \frac{T_1 - T_{w2}}{T_{w1} - T_{w2}}, \quad \theta_2 = \frac{T_2 - T_{w2}}{T_{w1} - T_{w2}}, \\ \phi = \frac{C}{C_w}, \quad P_1 = -\frac{h^2}{\mu_1\tilde{u}_1}\frac{\partial p}{\partial x}, \quad P_2 = -\frac{h^2}{\mu_2\tilde{u}_2}\frac{\partial p}{\partial x}, \quad Gr_1 = \frac{g\beta_1(T_{w1} - T_{w2})h^3}{\nu_1^2}, \quad Re_1 = \frac{\tilde{u}_1 h}{\nu_1}, \\ Gr_2 = \frac{g\beta_2(T_{w1} - T_{w2})h^3}{\nu_2^2}, \quad Re_2 = \frac{\tilde{u}_2 h}{\nu_2}, \end{cases} \tag{7}$$

where $\tilde{u}_i$ is the average velocity. The non-dimensional equations after dropping asterisks become

(i) Region-I ($0 \leqslant y \leqslant 1$):

$$\frac{\mathrm{d}^2 u_1}{\mathrm{d}y^2} + P_1 + 6\Delta_1 \frac{d^2 u_1}{dy^2}\left(\frac{du_1}{dy}\right)^2 + \lambda_1 \theta_1 = 0, \tag{8}$$

$$\frac{\mathrm{d}^2 \theta_1}{\mathrm{d}y^2} + Pr_1 \delta_1 \theta_1 + \Gamma_1 \left[\left(\frac{du_1}{dy}\right)^2 + 2\Delta_1 \left(\frac{du_1}{dy}\right)^4\right] = 0. \tag{9}$$

(ii) Region-II ($-1 \leqslant y \leqslant 0$):

$$\frac{\mathrm{d}^2 u_2}{\mathrm{d}y^2} + P_2 + 6\Delta_2 \frac{d^2 u_2}{dy^2}\left(\frac{du_2}{dy}\right)^2 + \lambda_2 \theta_2 = 0, \tag{10}$$

$$\frac{\mathrm{d}^2 \theta_2}{\mathrm{d}y^2} + \Gamma_2 \left[\left(\frac{du_1}{dy}\right)^2 + 2\Delta_2 \left(\frac{du_1}{dy}\right)^4\right] + Pr_2 \left[N_b \frac{\mathrm{d}\theta_2}{\mathrm{d}y}\frac{\mathrm{d}\phi}{\mathrm{d}y} + N_t \left(\frac{\mathrm{d}\theta_2}{\mathrm{d}y}\right)^2 + \delta_2 \theta_2\right] = 0, \tag{11}$$

$$\frac{\mathrm{d}^2 \phi}{\mathrm{d}y^2} + \frac{N_t}{N_b}\frac{\mathrm{d}^2 \theta_2}{\mathrm{d}y^2} = 0. \tag{12}$$

In the above equations, the parameters λ_i, Pr_i, N_b, N_t, Δ_i and Γ_i are the mixed convection parameters, the Prandtl numbers, the Brownian motion parameter, the thermophoresis parameter, the non-Newtonian coefficient and the Eckert number in the region-I and region-II, respectively, defined by

$$\lambda_1 = \frac{Gr_1}{Re_1}, \quad \lambda_2 = \frac{Gr_2}{Re_2}, \quad Pr_i = \frac{\nu_i}{\alpha_i}, \quad N_b = \frac{\tau D_B C_w}{\nu_2}, \quad N_t = \frac{\tau D_T (T_{w1} - T_{w2})}{\nu_2 T_{w2}} \tag{13}$$

$$\Delta_1 = \frac{\gamma_1 \tilde{u}^2}{\mu_1 h^2}, \quad \Delta_2 = \frac{\gamma_2 \tilde{u}^2}{\mu_2 h^2}, \quad \Gamma_1 = \frac{\mu_1 \tilde{u}^2}{k(T_{w1} - T_{w2})}, \quad \Gamma_2 = \frac{\mu_2 \tilde{u}^2}{k(T_{w1} - T_{w2})}. \tag{14}$$

Here, δ_1 and δ_2 are the heat source/sink parameter in the region-I and II, respectively, and

$$\delta_1 = \frac{Q_1 h_1^2}{\rho_1 C_p \nu_1}, \quad \delta_2 = \frac{Q_2 h_2^2}{\rho_2 C_p \nu_2}.$$

The corresponding boundary conditions in non-dimensional form are

$$\begin{cases} u_2(y) = 0, \quad \theta_2(y) = 0, \quad \phi(y) = 1 & \text{at } y = -1, \\ \left.\begin{array}{l} u_1(y) = u_2(y), \quad \theta_1(y) = \theta_2(y), \quad \phi(y) = 0, \\ \left[\frac{\mathrm{d}u_1}{\mathrm{d}y} + 2\Delta_1\left(\frac{\mathrm{d}u_1}{\mathrm{d}y}\right)^3\right] = \mu\left[\frac{\mathrm{d}u_2}{\mathrm{d}y} + 2\Delta_2\left(\frac{\mathrm{d}u_2}{\mathrm{d}y}\right)^3\right], \\ \frac{\mathrm{d}\theta_1}{\mathrm{d}y} = \frac{1}{k}\frac{\mathrm{d}\theta_2}{\mathrm{d}y}, \end{array}\right\} & \text{at } y = 0, \quad . \\ u_1(y) = 0, \quad \theta_1(y) = 1, & \text{at } y = 1, \end{cases} \tag{15}$$

where the ratios of the absolute viscosities and thermal conductivities are defined by

$$\mu = \frac{\mu_2}{\mu_1}, \quad k = \frac{k_1}{k_2}. \tag{16}$$

The additional conditions related to the mass flux conservation at any cross section in the channel read

$$\int_{-1}^{0} u_1(y)\, dy = 1 \tag{17}$$

and

$$\int_{0}^{1} u_2(y)\, dy = 1. \tag{18}$$

Noted that the pressure gradients P_1 and P_2 are unknown constants in Eqs. (8) and (10), since we have two additional Eqs. (17) and (18). Instead of solving the original Eqs. (8)–(12), we first differentiate Eqs. (8) and (10) w.r.t to the independent variable y: (i) Region-I ($0 \leqslant y \leqslant 1$):

$$\frac{\mathrm{d}}{dy}\left(\frac{\mathrm{d}^2 u_1}{\mathrm{d}y^2} + P_1 + 6\Delta_1 \frac{d^2 u_1}{dy^2}\left(\frac{du_1}{dy}\right)^2 + \lambda_1 \theta_1\right) = 0. \tag{19}$$

(ii) Region-II ($-1 \leqslant y \leqslant 0$):

$$\frac{\mathrm{d}}{dy}\left(\frac{\mathrm{d}^2u_2}{\mathrm{d}y^2}+P_2+6\Delta_2\frac{d^2u_2}{dy^2}\left(\frac{du_2}{dy}\right)^2+\lambda_2\theta_2\right)=0 \tag{20}$$

and then solve Eqs. (19), (9) for the region-I and (20), (11), (12) for the region-II, subject to the boundary conditions (15), (17) and (18), respectively, by means of the HAM-based Mathematica package BVPh 2.0. Thereafter, the values of P_1 and P_2 are given by the original Eqs. (8) and (10), respectively.

3. Analytic solutions given by the HAM

As a kind of analytic approximation method for highly nonlinear problems, the HAM has attracted the attention of many researchers: in the past two decades it has been successfully applied to solve lots of nonlinear problems in science, finance and engineering. To simplify the applications of the HAM, a few packages have been developed. In 2012, Liao [39] issued the HAM-based package BVPh 1.0 for nonlinear boundary-value/eigenvalue problems with singularity, multi-point boundary conditions and multiple solutions, governed by one ordinary differential equation (ODE). Currently, Zhao and Liao [40] issued its new version BVPh 2.0 for coupled nonlinear ODEs. By means of the Mathematica package BVPh 2.0, the system of the coupled nonlinear ODEs (19), (9), (20), (11) and (12), subject to the boundary conditions (15), (17) and (18), can be easily solved in the frame of the HAM, as shown below.

To shorten the length of the paper, we just describe the things necessary for the BVPh 2.0, but rather briefly. For details about the HAM and BVPh 2.0, please refer to Liao [39,40]. In the framework of the HAM, the solutions $u_i(y),\ \theta_i(y)$ and $\phi(y)$ can be expressed explicitly by an infinite series in the form

$$u_i(y)=\sum_{k=0}^{+\infty}u_{i,k}(y),\quad \theta_i(y)=\sum_{k=0}^{+\infty}\theta_{i,k}(y),\quad \phi(\eta)=\sum_{k=0}^{+\infty}\phi_k(y)\quad (i=1,2), \tag{21}$$

where $u_{i,k}(y),\ \theta_{i,k}(y),\ \phi_k(y)$ are governed by the so-called high-order deformation equations, which are linear and dependent upon a linear operator, called the auxiliary linear operator. The additional Eqs. (17) and (18) describing the closure property for channel flows will be incorporated as additional boundary conditions. These additional boundary conditions will be used to determine the unknown pressure constants in (8) and (10) for the known values of all other physical parameters. We have differentiated Eq. (8) and Eq. (10) with respect to y and together with the 12 boundary conditions, the system of coupled non-linear system of ODEs are solved by BVPh 2.0. In essence, the HAM transfers a nonlinear problem into an infinite number of linear sub-problems. However, the HAM provides us great freedom to choose the equation-type of these linear sub-problems and the base-functions of their solutions. For simplicity, the BVPh 2.0 needs to input the governing equations and boundary conditions, and choose proper initial guess of solution and auxiliary linear operators for these linear sub-problems.

In the frame of the HAM, one has great freedom to choose the auxiliary linear operator. Since the solutions are in a finite domain, they can be expressed by the polynomial functions. Thus, we choose the auxiliary linear operators

$$\mathcal{L}_1[u(y)]=\frac{\mathrm{d}^3u}{\mathrm{d}y^3} \tag{22}$$

for the high-order deformation equations corresponding to the Eqs. (19), (20), and

$$\mathcal{L}_2[u(y)]=\frac{\mathrm{d}^2u}{\mathrm{d}y^2} \tag{23}$$

for Eqs. (9), (11) and (12), respectively. The auxiliary linear operators possess the properties

$$\mathcal{L}_1[C_0+C_1y+C_2y^2]=0 \tag{24}$$

and

$$\mathcal{L}_2[C_0+C_1y]=0, \tag{25}$$

respectively, where $C_0,\ C_1$ and C_2 are constants to be determined.

Besides, in the frame of the HAM, we also have freedom to choose the initial guess of the solution. Considering the boundary conditions, we choose the following initial approximation

$$u_{1,0}(y)=\frac{3}{2}(1-y^2), \tag{26}$$

$$u_{2,0}(y)=\frac{3}{2}(1-y^2), \tag{27}$$

$$\theta_{1,0}(y)=\frac{1}{Kh}y+\left(1-\frac{1}{Kh}\right)y^2, \tag{28}$$

$$\theta_{2,0}(y)=y^2+y, \tag{29}$$

$$\phi_0(y)=\frac{3}{2}y^2+\frac{1}{2}y. \tag{30}$$

Table 1
Averaged squared residual errors using $\hbar_1 = -0.15$, $\hbar_1 = -1.20$, $\hbar_3 = -0.46$ whereas $\lambda_1 = \lambda_2 = \mu = Pr_1 = Pr_2 = 1$, $N_b = N_t = \Delta_1 = \Delta_2 = \Gamma_1 = \Gamma_2 = k = 0.1$.

m	20	40	60
P_1	5.1297	5.1291	5.1291
P_2	5.8231	5.8176	5.8176
$\mathcal{E}_m^{u_1}$	28.57×10^{-2}	12.47×10^{-4}	4.38×10^{-6}
$\mathcal{E}_m^{\theta_1}$	8.48×10^{-8}	2.39×10^{-11}	1.83×10^{-14}
$\mathcal{E}_m^{u_2}$	35.55×10^{-2}	16.0×10^{-4}	6.37×10^{-14}
$\mathcal{E}_m^{\theta_2}$	9.01×10^{-8}	2.78×10^{-11}	2.24×10^{-14}
$\mathcal{E}_m^{\phi}$	9.92×10^{-8}	1.37×10^{-11}	8.48×10^{-15}
$\mathcal{E}_m^{t}$	64×10^{-2}	29×10^{-4}	10×10^{-6}

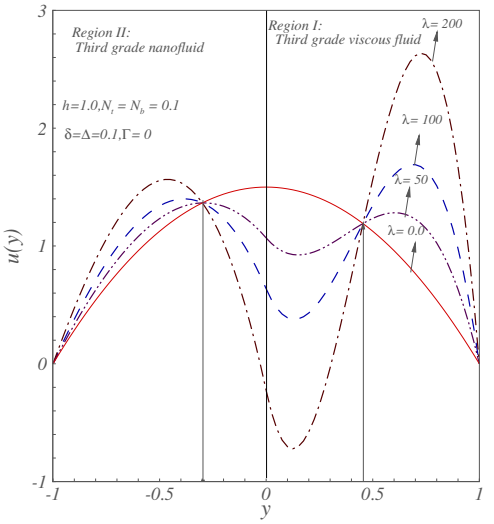

Fig. 2. Graphs of the velocity profile for different values of Lambda.

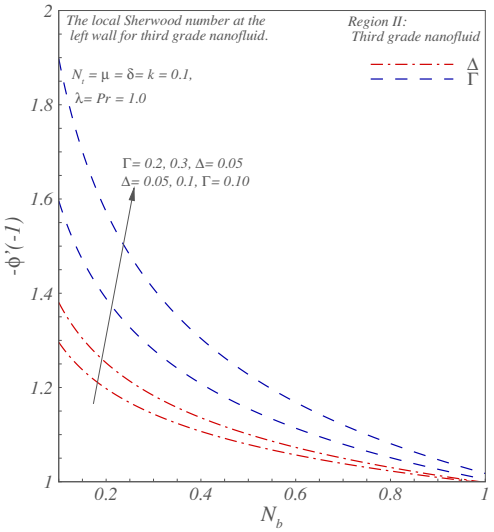

Fig. 3. Graphs of the local Sherwood number for N_b with different values of Δ and Γ.

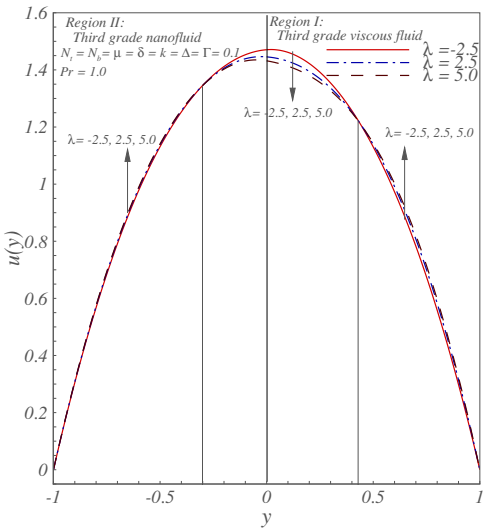

Fig. 4. Graphs of $u(y)$ for different λ.

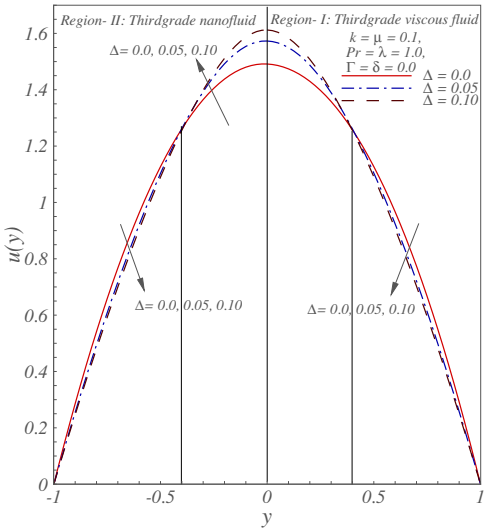

Fig. 5. Graphs of $u(y)$, $\theta(y)$ and $\phi(y)$ for different Δ.

Using the linear auxiliary operator (22), (23) and the initial approximations (26)–(30), the coupled nonlinear ODEs (19), (20), (9), (11) and (12), subject to the boundary conditions (15), (17) and (18), can be solved directly by means of the Mathematica package BVPh 2.0.

Unlike other analytic approximation methods, the HAM introduces the so-called "convergence-control parameter" to guarantee the convergence of solution series. In fact, it is the "convergence-control parameter" that differs the HAM from all other analytic methods. The "convergence-control parameters" have no physical meanings, and their optimal values can be determined by the minimum of residual square of governing equations, as pointed out by Liao [37].

Since there are five governing equations for the five unknown functions, we have five convergence-control parameters $c_0^{u_1}$, $c_0^{u_2}$, $c_0^{\theta_1}$, $c_0^{\theta_2}$, c_0^{ϕ}. For simplicity, we assume,

$$c_0^{u_1} = c_0^{u_2} = \hbar_1, \tag{31}$$

$$c_0^{\theta_1} = c_0^{\theta_2} = \hbar_2, \tag{32}$$

$$c_0^{\phi} = \hbar_3. \tag{33}$$

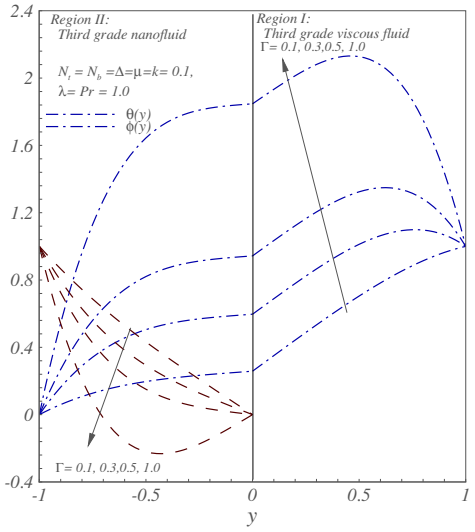

Fig. 6. Graphs of $\theta(y)$ and $\phi(y)$ for different Γ.

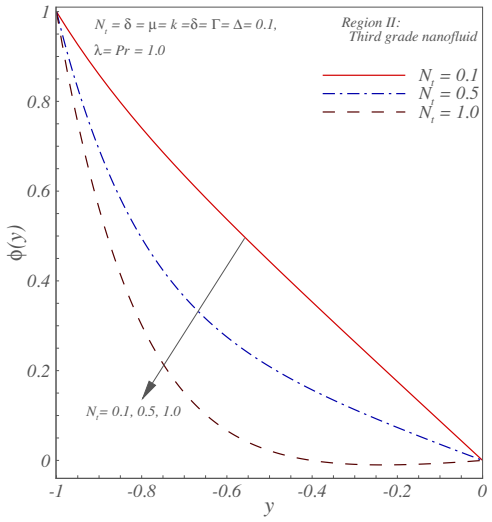

Fig. 7. Graphs of $\phi(y)$ for different N_t.

Let $\mathcal{E}_m^{u_1}$, $\mathcal{E}_m^{u_2}$, $\mathcal{E}_m^{\theta_1}$, $\mathcal{E}_m^{\theta_2}$, $\mathcal{E}_m^{\phi}$ denote the residual squares of the five governing equations at the mth-order of approximation, respectively, and $\mathcal{E}_m^t$ their sum. The optimal value of the convergence-control parameter $\hbar_1$ is determined by the minimum of the total residual square $\mathcal{E}_m^t$.

For example, let us consider the case $\lambda_1 = \lambda_2 = Pr_1 = Pr_2 = \mu = 1,\ N_b = N_t = \Delta_1 = \Delta_2 = \Gamma_1 = \Gamma_2 = k = 0.1$. In order to compute optimal convergence-control parameter $\hbar_1,\ \hbar_2$ and $\hbar_3$ we minimize total average squared residual for Eqs. (19), (20), (9), (11) and (12), by directly employing the command **GetOptiVar** of the BVPh 2.0. The HAM approximations are substituted in Eqs. (8) and (10) to determine the unknown pressure constants. Using the optimal convergence control parameters corresponding to 5-th order of approximation i.e. the optimal convergence-control parameter $\hbar_1 = -0.15,\ \hbar_2 = -0.1.20$ and $\hbar_1 = -0.46$, not only the total error but also the residual squares for each equation decays: the total error decays to the level 10×10^{-6} at the 60th-order of approximation, also P_1 and P_2 converges to a unique value, i.e. $P_1 = 5.1297$ and $P_2 = 5.8231$, as shown in Table 1. Thus, by means of the BVPh 2.0, we indeed gain an accurate analytic approximation for the considered case.

4. Results and discussion

For different physical parameters, we can use the HAM-based Mathematica package BVPh 2.0 [40] to gain accurate results in a similar way. In this section, the influence of the physical parameters on the flow and heat/mass transfer is investigated in details.

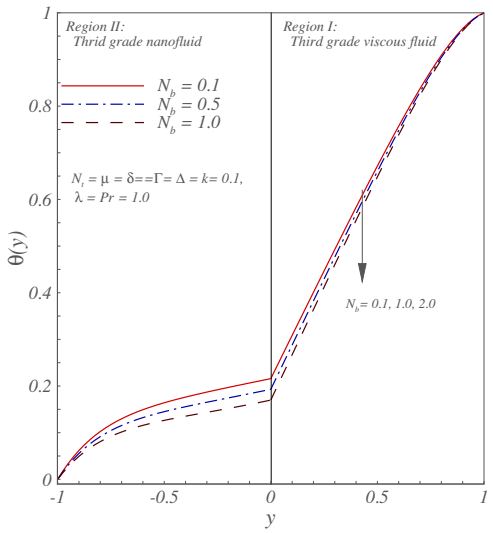

Fig. 8. Graphs of $\theta(y)$ for different N_b.

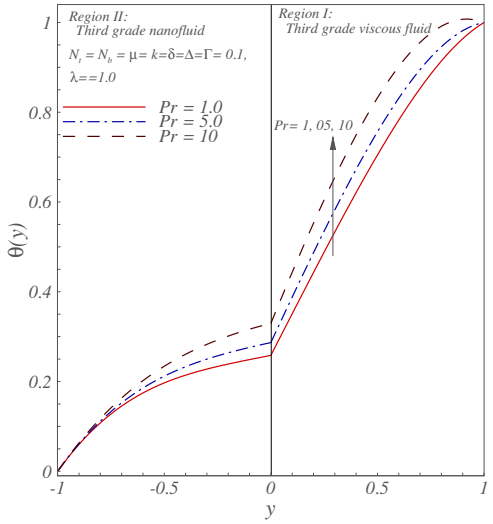

Fig. 9. Graphs of $\theta(y)$ for different Pr.

Figs. 2–11 depict interesting features of velocity, temperature, concentration profiles, local skin friction coefficient and local Nusselt number. Graphical analysis has been carried out for different values of Brownian motion parameter (N_b), thermophoresis parameter (N_t), mixed convection parameter (λ), Prandtl number (Pr), non-dimensional coefficient (Γ) and non-Newtonian third grade fluid parameter (Δ).

Fig. 2 shows the clear fluid and nano-fluid velocity profiles in region-I and region-II for different values of the mixed convection parameter λ in the absence of viscous dissipation. The physical parameter $\lambda = \frac{Gr}{Re}$ describes the mixed convection. The limiting values $\lambda \to 0$ and $\lambda \to \infty$ correspond to the forced and free convection, respectively. In the absence of mixed convection parameter i.e. $\lambda = 0$, the externally induced flow is parabolic and attains its maximum value at the interface. The increase in the values of λ results in significant buoyancy effects, which leads to the increase in the velocity profiles adjacent to the heated right wall channel. It can be seen from Fig. 2 that the buoyancy parameter causes an adverse pressure gradient, which results in the separation of the flow so that the flow starts reversing its direction. The extent of the reversed flow region falls short of $y = 0.45$ in the clear fluid and $y = -0.30$ in the nano-fluid, respectively. The buoyancy effects are dominant in the clear fluid region, i.e. the magnitude of change due to the mixed convection parameter is larger in the clear fluid than in the nano-fluid.

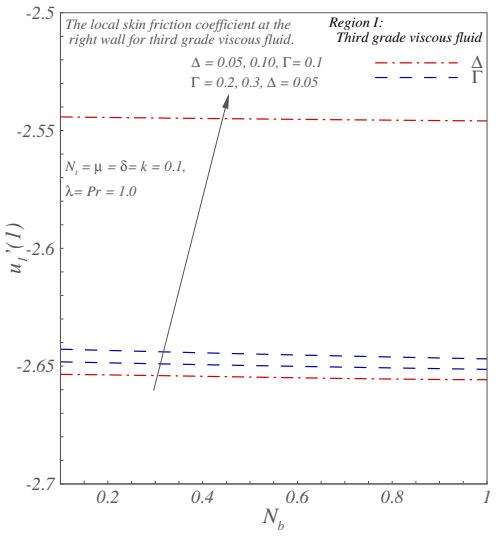

Fig. 10. Graphs of the local skin friction for N_b at the right wall with different values of Δ and Γ.

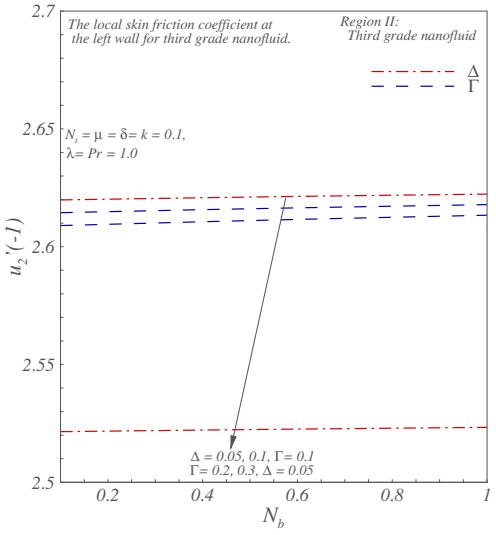

Fig. 11. Graphs of the local skin friction at the left wall for N_b with different values of Δ and Γ.

The influence of the physical parameters Δ and Γ on the local Sherwood number at the left wall are depicted in Fig. 3. It is observed that at the left wall the local Sherwood number is a decreasing function of N_b. The increase in either Δ or Γ leads to the increase of the mass transfer at the left wall.

Fig. 4 displays the influence of the mixed convection parameter on the fluid flow in the presence of viscous dissipation. The increase of λ results in the increase of the buoyancy and hence the increase of the velocity profile near the walls but near the interface the flow decreases with the increase in λ. From Figs. 2 and 4, we may conclude that the mixed convection parameter can effectively control the velocity profile. For brevity, in the following results, we use the fixed values of the physical parameters $\lambda_1 = \lambda_2 = \lambda,\ \Delta_1 = \Delta_2 = \Delta,\ \Gamma_1 = \Gamma_2 = \Gamma,\ Pr_1 = Pr_2 = Pr$.

The influence of the third-grade non-Newtonian parameter Δ on the fluid velocity is shown in Fig. 5. It is found that the velocity increases in the vicinity of the interface with the increase in Δ, due to the shear thinning behavior of the third-grade fluid.

Fig. 6 illustrates the influence of the non-dimensional parameter Γ on the temperature and nano-particle volume fraction. The increase of Γ results in the increase of the temperature profiles. The increase in the temperature profile is due to the heat energy stored in the fluid. The nano-particle volume fraction decreases with the increase of Γ.

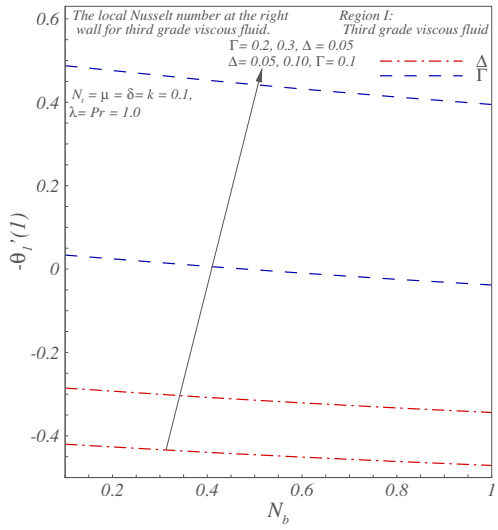

Fig. 12. Graphs of the local Nusselt number for N_b at the right wall with different values of Δ and Γ.

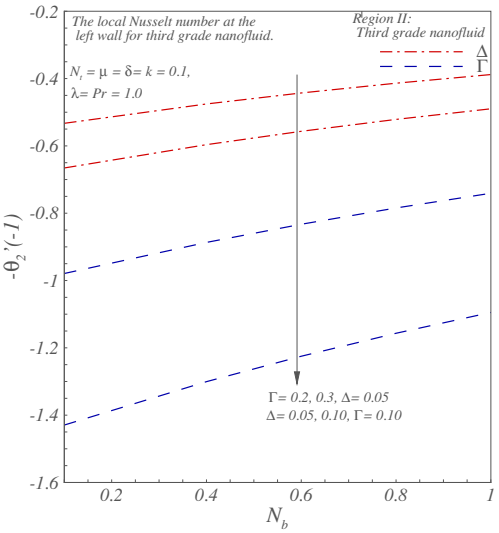

Fig. 13. Graphs of the local Nusselt number for N_b at the left wall with different values of Δ and Γ.

The influence of the thermophoresis parameter on the nano-particle volume fraction is shown in Fig. 7. It is found that the increase in the thermophoresis parameter considerably alters the nano-particle volume fraction. Besides, the increase in N_t reduces the concentration profile. It is due to the presence of temperature difference in the thermophoresis parameter that decreases the mixed convection mass transfer.

The continuous collision between the nano-particles and the molecules of the base fluid within the base fluid is called the Brownian motion. Fig. 8 depicts that the Brownian motion parameter decreases the fluid temperature throughout the channel.

The influence of Prandtl number on the fluid temperature are as shown in Fig. 9. The increase in Prandtl number leads to the increase of the temperature profile in clear fluid region.

Figs. 10 and 11 have been plotted to show the influences of Δ and Γ on the local skin friction coefficient at the left and right walls, respectively. At the left wall in the nano-fluid region, the local skin friction is a decreasing function of N_b, whereas at the right wall in the clear fluid region the local skin friction is an increasing function of N_b. The increase in either Δ or Γ leads to enhance the momentum transfer at the right wall, while quite the opposite is noticed at the right wall.

Figs. 12 and 13 illustrate the influence of Δ and Γ on the local Nusselt number at the left and right walls, respectively. At the left wall in the nano-fluid region the local Nusselt number is an increasing function of N_b, whereas at the right wall in the

clear fluid region the local Nusselt number is a decreasing function of N_b, respectively. The increase in either Δ or Γ leads to the deceleration of the heat transfer at the left wall, while quite opposite is true at the right wall.

5. Conclusions

The flow and heat transfer of non-Newtonian third-grade nano-fluid layer adjacent to a non-Newtonian third-grade clear fluid layer in a vertical channel is studied analytically. The resulting multi-point boundary-value problem governed by five coupled nonlinear ODEs is solved by means of an easy-to-use Mathematica package BVPh 2.0 based on the HAM. The influences of the physical parameters Δ, Γ, N_b, N_t and λ on the fluid flow, temperature, concentration profiles, the local skin frictions, the local Nusselt number and the local Sherwood number are studied in details. Our convergent analytic results indicate that:

(1) For sufficiently large values of mixed convection parameter, reversed flow is observed throughout the channel.
(2) Increase in λ, enhances the fluid flow near the walls but fluid velocity decreases in the vicinity of interface.
(3) Increase in N_b results in the decrease of the temperature whereas temperature increases with the increase in Pr.
(4) Increase in N_t leads to the decrease of the concentration profiles.
(5) At the left wall, the local skin friction increases with the increase in N_b but decreases with the increase in either Δ or Γ, while quite opposite is true at the right wall of channel.
(6) At the left wall, the local Sherwood number decreases with the increase in N_b but increases with the increases in either Δ or Γ.
(7) At the left wall, the local Nusselt number increases with the increase in N_b but decrease with the increases in either Δ and Γ, while quite opposite is true at the right wall.

All of these deepen and enrich our understanding about the considered boundary-layer flows. It also illustrates the general validity and power of the HAM-based Mathematica package BVPh 2.0 for complicated boundary-layer flows.

Acknowledgments

This work is funded by the Deanship of Scientific Research (DSR), King Abdulaziz University (KAU) under Grant No. 37-130-35-HiCi. The authors, therefore, acknowledge technical and financial support of KAU. It is also partially supported by State Key Laboratory of Ocean Engineering (Approval No. GKZD010063) and National Natural Science Foundation of China (Approval Nos. 11272209 and 51209136).

References

[1] E.M. Sparrow, R. Eichhom, J.C. Gregg, Combined forced and free convection in a boundary layer flow, Phys. Fluids 2 (1959) 319–328.
[2] E.M. Sparrow, J.C. Gregg, Buoyancy effects in forced convection flow and heat transfer, J. Appl. Mech. 26 (1959) 133–138.
[3] L.N. Tao, On combined free and forced convection in channels, ASME J. Heat Transfer 82 (1960) 233–238.
[4] A.A. Szewczyk, Combined forced and free convection laminar flow, J. Heat Transfer 86 (1964) 501–507.
[5] J.H. Merkin, The effect of buoyancy forces on the boundary layer flow over a semi-infinite vertical plate in a uniform stream, J. Fluid Mech. 35 (1969) 439–450.
[6] K.R. Rajgopal, T.Y. Na, Natural convection flow of a non-newtonian fluid between two vertical flat plates, Acta Mech. 54 (1985) 239–246.
[7] W. Aung, G. Worku, Developing flow and flow reversal in a vertical channel with asymmetric wall temperature, ASME J. Heat Transfer 108 (1986) 299–304.
[8] W. Aung, G. Worku, Theory of fully developed, combined convection including flow reversal, ASME J. Heat Transfer 108 (1986) 485–488.
[9] M. Massoudi, I. Christie, Natural convection fluid of a non-Newtonian fluid between two concentric vertical cylinders, Acta Mech. 82 (1990) 11–19.
[10] A. Barletta, Fully developed mixed convection and flow reversal in a vertical rectangular duct with uniform wall heat flux, Int. J. Heat Mass Transfer 45 (2002) 641–654.
[11] K. Boulama, N. Galanis, Analytical solution for fully developed mixed convection between parallel vertical plates with heat and mass transfer, ASME J. Heat Transfer 126 (2004) 381–387.
[12] I.G. Baoku, B.I. Olajuwon, Heat and mass transfer on a MhD third grade fluid with partial slip flow past an infinite vertical insulated porous plate in a porous medium, Int. J. Heat Fluid Flow 40 (2013) 81–88.
[13] T. Hayat, A.H. Kara, Couette flow of a third-grade fluid with variable magnetic field, Math. Comput. Model. 43 (2006) 132–137.
[14] T. Hayat, F. Shahzad, M. Ayub, Analytical solution for the steady flow of the third grade fluid in a porous space, Appl. Math. Model. 31 (2007) 2424–2432.
[15] T. Hayat, M.A. Farooq, T. Javed, M. Sajid, partial slip effects on the flow and heat transfer characteristics in a third grade fluid, Nonlinear Anal.: Real World Appl. 10 (2009) 745–755.
[16] T. Hayat, S. Hina, A.A. Hendi, S. Asghar, Effect of wall properties on the peristaltic flow of a third grade fluid in a curved channel with heat and mass transfer, Int. J. Heat Mass Transfer 54 (2011) 5126–5136.
[17] S.S. Okoya, Disappearance of criticality for third grade fluid with Reynold's model viscosity in a flat channel, Int. J. Non-linear Mech. 46 (2011) 1110–1115.
[18] B. Sahoo, Flow and heat transfer of a third grade fluid past an exponentially stretching sheet with partial slip boundary condition, Int. J. Heat Mass Transfer 54 (2011) 5010–5019.
[19] C. Beckermann, S. Ramadyani, R. Viskanta, Natural convection flow and heat transfer between a fluid layer and porous layer inside a rectangular enclosure, J. Heat Transfer 109 (1977) 363–370.
[20] T. Kimura, N. Heya, M. Takeuchi, H. Isomi, Natural convection heat transfer phenomena in an enclosure filled with two stratified fluids, Jpn. Soc. Mech. Eng. (B) 52 (1986) 617–625.

[21] M.S. Malashetty, J.C. Umavathi, J.P. Kumar, Magnetoconvection of two-immiscible fluids in a vertical enclosure, J. Heat Mass Transfer 42 (2006) 977–993.
[22] J.P. Kumar, J.C. Umavathi, A.J. Chamkha, I. Pop, Fully-developed free convective flow of micropolar and viscous fluids in a vertical channel, J. Appl. Math. Model. 34 (2010) 1175–1186.
[23] J.C. Umavathi, I.C. Liu, J.P. Kumar, D.S. Meera, Unsteady flow and heat transfer of porous media sandwiched between viscous fluids, J. Appl. Math. Mech. Engl. 31 (12) (2010) 1497–1516.
[24] D. Nikodijevic, Z. Stamenkovic, D. Milenkovic, B. lagojevic, J. Nikodikevic, Flow and heat transfer of two immiscible fluids in the presence of uniform inclined magnetic field, J. Math. Prob. Eng. (2011), http://dx.doi.org/10.1155/2011/132302. 18p (Article ID 132302).
[25] J.K. Parthab, J.C. Umavathi, M.B. Basavaraj, Mixed convection of magneto hydrodynamic and viscous fluids in a vertical channel, Int. J. Non-linear Mech. 46 (2011) 278–285.
[26] S.U. Choi, Enhancing thermal conductivity of fluids with nanoparticle, ASME J. Develop. Appl. Non-Newtonian Flows 66 (1995) 99–105 (FED 231/MD).
[27] S.K. Das, S.U. Choi, W. Yu, T. Pardeep, Nanofluids: Science and Technology, Wiley, New Jersey, 2007.
[28] X.Q. Wang, A.S. Mujundar, A review on nanofluids – Part I: Theoretical and numerical investigations, Braz. J. Chem. Eng. 25 (2008) 613–630.
[29] A.V. Kuznetsov, D.A. Nield, Natural convective boundary layer flow of a nanofluid past a vertical plate, Int. J. Therm. Sci. 49 (2010) 243–247.
[30] H. Xu, I. Pop, Fully developed mixed convection flow in a vertical channel filled with nanofluids, Int. Commun. Heat Mass Transfer 39 (2012) 1086–1092.
[31] T. Gorsan, I. Pop, Fully developed mixed convection in a vertical channel filled by a nanofluid, ASME J. Heat Transfer 134 (2012) 1–5.
[32] H. Xu, T. Fan, I. Pop, Analysis of mixed convection flow of a nanofluid in a vertical channel with the Buongiorno mathematical model, J. Int. Commun. Heat Mass Transfer 44 (2013) 15–22.
[33] R.A.V. Gorder, K.V. Prasad, K. Vajravelu, Convective heat transfer in the vertical channel flow of a clear fluid adjacent to a nanofluid layer: a two-fluid model, J. Heat Mass Transfer (2012), http://dx.doi.org/10.1007/s00231-021-0973-2.
[34] U. Farooq, Z. Lin, Nonlinear heat transfer in a two-layer flow with nanofluids by OHAM, J. Heat Transfer (2013), http://dx.doi.org/10.1115/1.4025432.
[35] K. Vajravelu, K.V. Prasad, S. Abbasbandy, Convective transport of nanoparticle in multi-layer fluid flow, Appl. Math. Mech. Eng. Ed. 34 (2) (2013) 177–188, http://dx.doi.org/10.1007/s104833-013-1662-6.
[36] S. Liao, A kind of approximate solution technique which does not depend upon small parameters (II) – an application in fluid mechanics, Int J. Non-linear Mech. 32 (1997) 815–822.
[37] S. Liao, An optimal homotopy-analysis approach for strongly nonlinear differential equations, J. Commun. Non-linear Sci. Numer Simul. 15 (2010) 2003–2016.
[38] S. Liao, Beyond Perturbation. Introduction to Homotopy Analysis Method, Chapman and Hall/CRC Press, Boca Raton, 2003.
[39] S. Liao, Homotopy Analysis Method in Nonlinear Differential Equations, Higher Education Press, Beijing, 2012.
[40] Y. Zhao, S. Liao, HAM-based package BVPh 2.0 for nonlinear boundary value problems, in: S. Liao (Ed.), Advances in Homotopy Analysis Method, World Scientific Press, 2013.
[41] J. Buongiorno, Convective transport in nano fluids, ASME J. Heat Transfer 128 (2006) 240–250.